ACADEMIA ROMÂNĂ
Revue Roumaine de Chimie
http://web.icf.ro/rrch/

Rev. Roum. Chim.,
2018, *63*(11), 1083-1091

APPLICATION OF 2D AND 3D SIMILARITY METHODS TO GSK-3 BENCHMARKING VALIDATION DATASET INCLUDING SELECTIVE AND NONSELECTIVE INHIBITORS

Luminita CRISAN, Daniela VARGA, Sorin AVRAM and Liliana PACUREANU*

Institute of Chemistry Timişoara of the Roumanian Academy, 24 Mihai Viteazul Ave., 300223 Timişoara, Roumania

Received July 24, 2018

In this work an *in silico* study based on 2D and 3D similarity methodologies and a benchmarking data set made up of experimentally confirmed actives including selective and nonselective inhibitors and inactives for glycogen synthase kinase 3 (GSK-3) was performed. The results obtained highlight the relevance of 3D shape and the so-called "color" features regarding actives prioritization in virtual screening assessment of GSK-3 inhibitors. The Color Score and Scaled Color coefficients delivered the best rankings in terms of 3D similarity search. The current analysis of bioactivity *versus* selectivity profiles can be of utility providing comprehensive insights into molecular prerequisites, which may facilitate the knowledge-based identification of novel active and selective compounds with appropriated pharmacological profile.

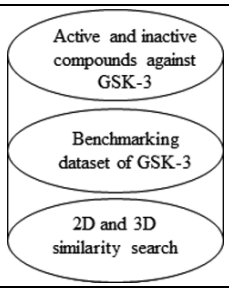

INTRODUCTION

Protein kinases are implicated in a number of cellular processes including cell apoptosis, growth, differentiation, etc.[1,2] Therefore, GSK-3 inhibitors are considered a valuable class of therapeutic agents.[3] A plethora of discoveries have been published in the field of rational design of drug-like inhibitors which bind to kinase ATP binding pocket.[4,5]

Glycogen synthase kinase 3 (GSK-3) is a serine/threonine protein kinase which is considered one of the most attractive therapeutic targets.[6-8] This kinase is encoded by two genes GSK3α and GSK3β, which share high overall sequence homology (85%).[9] The chemical space of GSK-3β inhibitors include a large structural variety of compounds such as indirubins, maleimides, aloisines paullones, hymenialdisine, etc.[10- 14] In recent years many computational investigations of GSK-3 inhibitors chemical space include QSAR, docking, pharmacophore modeling, similarity search have been reported.[15-33]

High affinity and selectivity are two of the most important properties of drug - like molecules.[34] The current analysis is focused on chemico-biological properties of GSK-3 inhibitors. We collected active (selective and nonselective) inhibitors against GSK-3 and included them in a benchmarking database.[33] We have chosen inhibitors of GSK-3 which were tested against related kinases: cyclin-dependent kinase 2 (CDK-2), cyclin-dependent kinase 4 (CDK-4) and protein kinase C (PKC).[33]

Our goal is to accomplish comprehensive virtual screening experiments based on 2D and 3D similarity to identify the specific arrangement of molecular features which are correlated to inhibition of GSK-3. Furthermore, we pursued the prioritization of actives in addition to inactives from benchmarking validation dataset. We applied 2D and 3D similarity search because the molecular fields are described from distinct perspectives and the chemical space is comprehensively covered having a great practical utility.[35-37] The employment

* Corresponding author: pacureanu@acad-icht.tm.edu.ro

of high-quality data sets based on experimentally validated inactives is indispensable in order to certificate a virtual screening methodology.[38,39] At the same time the availability of confirmed chemical and biological data for a suitable number of molecules is necessary.[39,40]

METHODS

Data set

For 2D and 3D similarity analysis we assembled a validation data set for GSK-3, consisting of active and inactive compounds.[33] Ten most potent GSK-3 inhibitors maleimide derivatives (Figure 1) were selected from the literature[41,42] and used as reference molecules for 2D and 3D similarity search.

The compounds with experimental activities against GSK-3, CDK-2, CDK-4 and PKC were picked from ChEMBL database,[43] Binding DB,[44] and reference[42] and were assembled into a database with 237 unique compounds, as shown in our published paper.[33] The distribution of experimental activities on active class were depicted in Figure 2.

Similarly, the inactive class was chosen from true inactives included in confirmatory PubChem assays against GSK-3β, AID434954, and against GSK-3α, AID 463203.[33,46] For inactive compounds, the simple physico-chemical property-space filtering relevant to drug likeness was applied in order to match the properties of active compounds (MW= 231÷625, HBA = 1÷7, HBD = 1÷7, 2dPSA = 45÷155, XLogP = -1.26÷6.2 and RBN = 0÷13), retaining 2016 inactive compounds.[33] Thereby, the similarity between actives and inactives in terms of simple physico-chemical descriptors is preserved.[33]

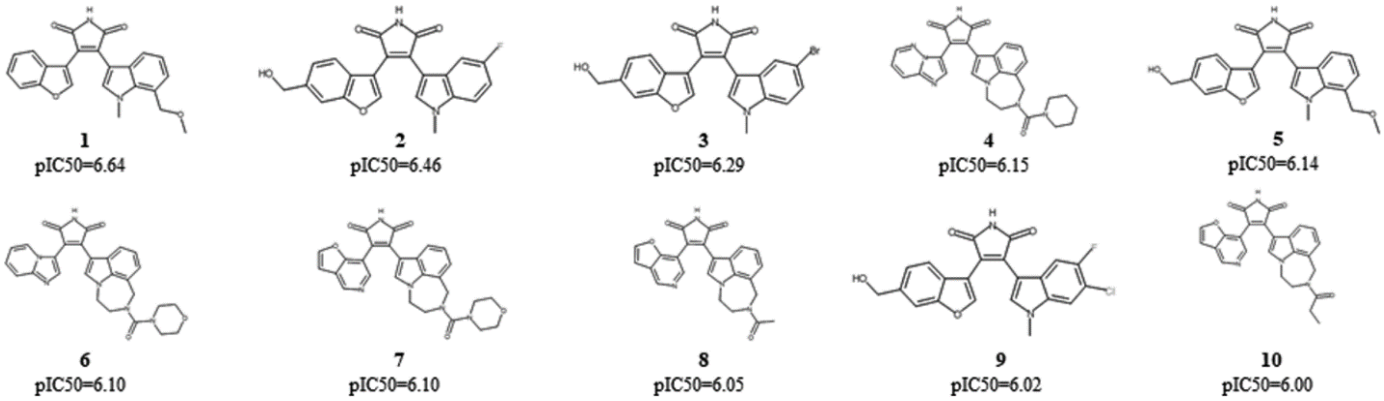

Fig. 1 – The query compounds used in 2D and 3D similarity search and their biological activities against GSK-3 converted to a logarithmic scale[45] (queries **1**, **2**, **3**, **5**, **9** – reference,[41] queries **4**, **6**, **7**, **8**, **10** – reference[42]).

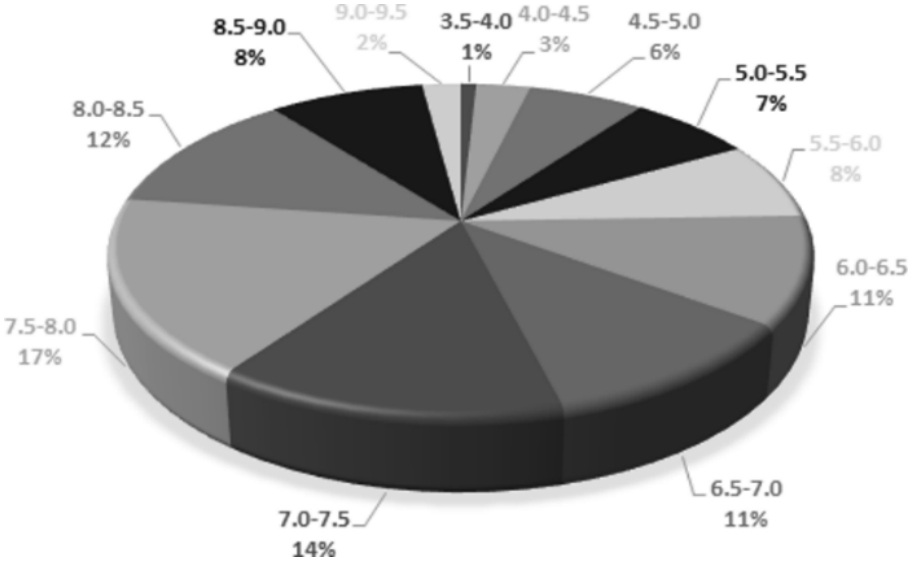

Fig. 2 – The distribution of biological activity converted to a logarithmic scale in the data set.

Thus, the application of our validation data set offer the possibility to assess actives against inactives to efficiently evaluate the discriminative power of 2D and 3D ligand-based virtual screening methods.

2D Similarity

181 2D-descriptors were calculated with FILTER software[47] from OpenEye package (http://www.eyesopen.com) and after that their values were mean-centered and scaled between 0 and 1. We calculated four 2D similarity association coefficients such as Tanimoto Jaccard, Dice, Fossum and Cosine Ochiai and four 2D distance coefficients including Mean Euclidean, Mean Manhattan, Mean Canberra and Divergence with our in house developed software entitled SSTICIv1 (Similarity Search Tool In ChemoInformatics).[48]

3D Similarity

Rapid overly of chemical structures (ROCS)[49-51] (http://www.eyesopen.com) is well known as the standard tool for ligand based virtual screening. 13 3D similarity coefficients based on shape, color and a combination between these two are included in ROCS:[49-51] Tanimoto Combo, Shape Tanimoto, Color Tanimoto, Scaled Color, Combo Score, Color Score, Fit Tversky Combo, Fit Tversky, Fit Color Tversky, Ref Tversky Combo, Ref Tversky, Ref Color Tversky, and Overlap similarity coefficients were computed.

Color Score measures the pharmacophore similarity by superposition of dummy atoms which characterize pharmacophores fields,[49] *i.e.*, implicitly Mills Dean force field describes six pharmacophore points: hydrogen bond donor, hydrogen bond acceptor, hydrophobic, anions, cations, and rings.[49] Ten similarity searches were carried out using ten queries (Figure 1) against the benchmarking dataset including 237 active and 2106 inactive compounds.[33]

Evaluation methods

The performance of similarity search in addition to retrieval of actives in terms of area under curve (AUC)[52] metric (see eq. 1) was estimated using another in-house developed program ETICI1.6 (Evaluation Tool In ChemInformatics).[53] The AUC provide information related to the number of actives recovered at the top of the hit list where AUC value of 1 indicates the perfect separation of actives at the top of the ranking list, whereas AUC of 0.5 denotes random distribution of actives and inactives.[52] In order to prove the performance of virtual screening methods, the early enrichment[54] (eq. 2) is commonly used. Early enrichment is calculated as the true positive rate (TPR) eq. (3) at 2, 5, and 10% of false positive rates (FPR) (eq. 4).

$$AUC = 1 - \frac{1}{TP + FN} \sum_{i=1}^{TP+FN} FPR_i \qquad (1)$$

$$TPR_x = TPR \text{ at } x\%\ FP, \text{ where } x = 2\%, 5\%, 10\% \qquad (2)$$

$$TPR = \frac{TP}{TP + FN} \qquad (3)$$

$$FPR = \frac{FP}{FP + TN} \qquad (4)$$

where TP denotes the true positives (correctly predicted actives), TN is true negatives (correctly predicted inactives), FP represents the false positives (incorrectly identified actives), FN designates the false negatives (incorrectly identified inactives), TPR stands for the fraction of correctly predicted actives (true positive rate), and FPR indicates the ratio of the mispredicted inactives.

RESULTS

2D similarity

First we analyzed the values registered for 2D Tanimoto coefficient, the standard in the field, to evaluate actives *versus* inactives in terms of physico-chemical similarity. The average for 2D Tanimoto values are consistently little higher for active *versus* inactive compounds. The smallest average difference between actives and inactives was observed for query **1** and the highest discrepancy was observed for queries **4** and **7** (see Table 1).

The analysis of AUC's values resulted from 2D similarity rankings was performed for active *versus* inactive compounds (validation data set). The performance of 2D descriptors in addition to retrieval of actives from decoys in terms of AUC metric is shown in Figure 3a. The average AUC scores for all coefficients, on actives-inactives data set are of 0.602. The 2D distance similarity coefficients show distinct trends over the queries,

but Mean Canberra and Divergence for queries **4**, **6** and **7**, display the highest AUC values. The Mean Manhattan for the same queries (**4**, **6** and **7**) show AUC values greater than 0.7. The performance of all queries is poor for this data set, but only Divergence and Mean Canberra for query **6** result in significant enrichment (AUC = 0.801/0.820), as well as in the case of Mean Canberra with query **4** (AUC = 0.818), whereas Mean Manhattan produce an AUC of only 0.711. The 2D association similarity coefficients display the highest AUC values for Dice coefficient for query **7** (0.713) and for query **6** (0.680). The higher AUC value for Tanimoto Jaccard coefficient was observed for query **6** (0.680). The query **8** produces an AUC of 0.571 for Cosine Occhiai and Fossum. The best average enrichment for all queries was observed for molecules **4** and **6** and equal only 0.685.

3D similarity

The average of 3D Shape Tanimoto values reflect the same trend as average of 2D Tanimoto values, with the highest difference between actives and inactives for query **1**, but in this case the smallest difference was registered for query **9** (see Table 2).

Figure 3b shows the variation of the AUC values obtained for the benchmarking data set. The simplest 3D similarity measures Fit Tversky and Shape Tanimoto display the lowest ranking performance. An average performance is showed by Combo Score and Tanimoto Combo, whereas the best retrieval of actives was provided by Color Score and Scaled Color. The molecules in the validation dataset are unsatisfactorily ranked by the shape, resulting that the discrimination between actives and inactives resulted only by applying molecular shape is not appropriate.

However, the best retrieval was obtained in the case of the coefficients containing color field Scaled Color and Color Score using query **2** AUC = 0.869, followed by query **3** AUC = 0.858, and query **9** AUC = 0.847. Clearly, the queries **4** and **1** exhibited lowest average and minimum AUC value (see Fig. 3). The largest discrepancies in terms of AUC occurred between Fit Tversky and Color Score 0.431 for query **2**. It results that not the shape, but pharmacophore features are mandatory to obtain high accuracy retrievals.

As expected the ranking performance of the 3D similarity method is superior to 2D similarity yielding higher AUC values. However, AUC register the overall improvement which covers up the early enrichment performance. In our experiments the highest early enrichments were obtained for Ref Tversky Combo (query **2** (59.916 at 2% FP, 65.401 at 5% FP, 70.042 at 10% FP) followed by queries **3** (57.806 at 2% FP, 64.135 at 5% FP, 69.198 at 10% FP) and query **9** (57.384 at 2% FP, 62.869 at 5% FP, 64.135 at 10% FP).

Significant differences arising from 2D and 3D similarity virtual screening experiments suggest that shape, conformational flexibility, and pharmacophore features, play essential roles regarding ligand binding to GSK-3. 3D similarity algorithm emerged as a satisfactorily precise and fast approach to detect potentially active compounds for GSK-3 form inactives. The superior performance of 3D similarity method which is supposed to embody more adequately various binding characteristics, is especially convenient for the enhancement of 2D virtually prescreened chemical collections.[55] As previously suggested molecular shape and physico-chemical pattern analysis can provide insightful information, *e.g.* a database of shape and pharmacophore signatures resulted from 3D representations of bioactive molecules.[30,33,56]

Table 1

Average 2D Tanimoto values for benchmarking set in relation to all queries

Query/ Data set	**1**	**2**	**3**	**4**	**5**	**6**	**7**	**8**	**9**	**10**	Average
Actives	0.956	0.957	0.945	0.921	0.956	0.920	0.920	0.954	0.954	0.950	0.943
Inactives	0.955	0.947	0.913	0.869	0.939	0.869	0.868	0.931	0.934	0.921	0.914

Table 2

Average 3D Shape Tanimoto values for benchmarking set in relation to all queries

Query/ Data set	**1**	**2**	**3**	**4**	**5**	**6**	**7**	**8**	**9**	**10**	Average
Actives	0.655	0.645	0.656	0.614	0.652	0.615	0.608	0.660	0.648	0.656	0.641
Inactives	0.555	0.577	0.589	0.526	0.570	0.534	0.529	0.585	0.589	0.578	0.563

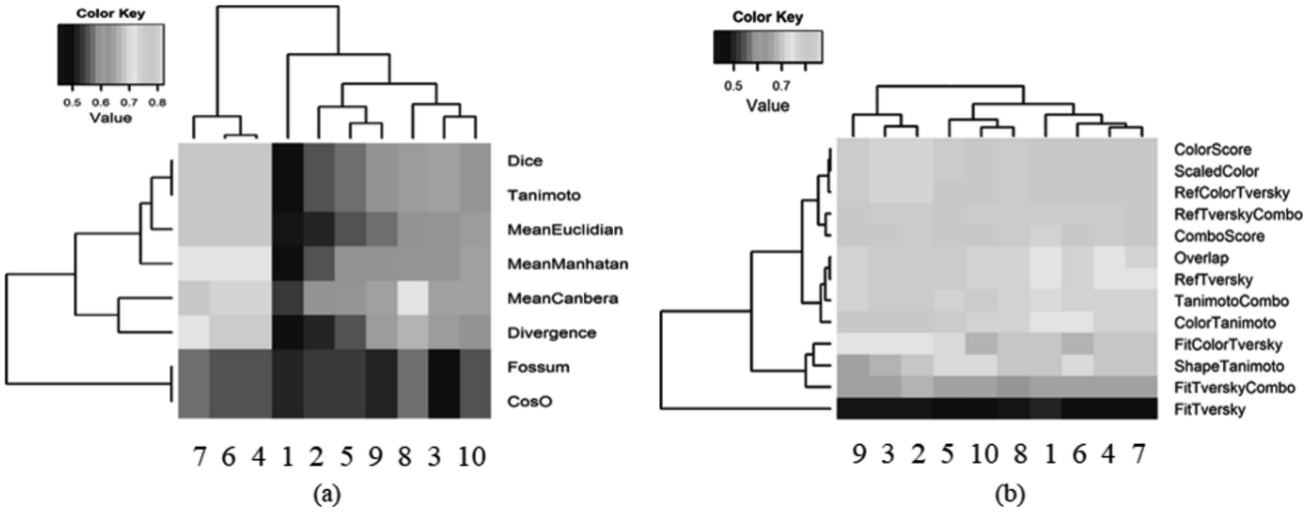

Fig. 3 – The heatmap of AUC's for 2D similarity search (a); The heatmap of AUC's for 3D similarity search (b).

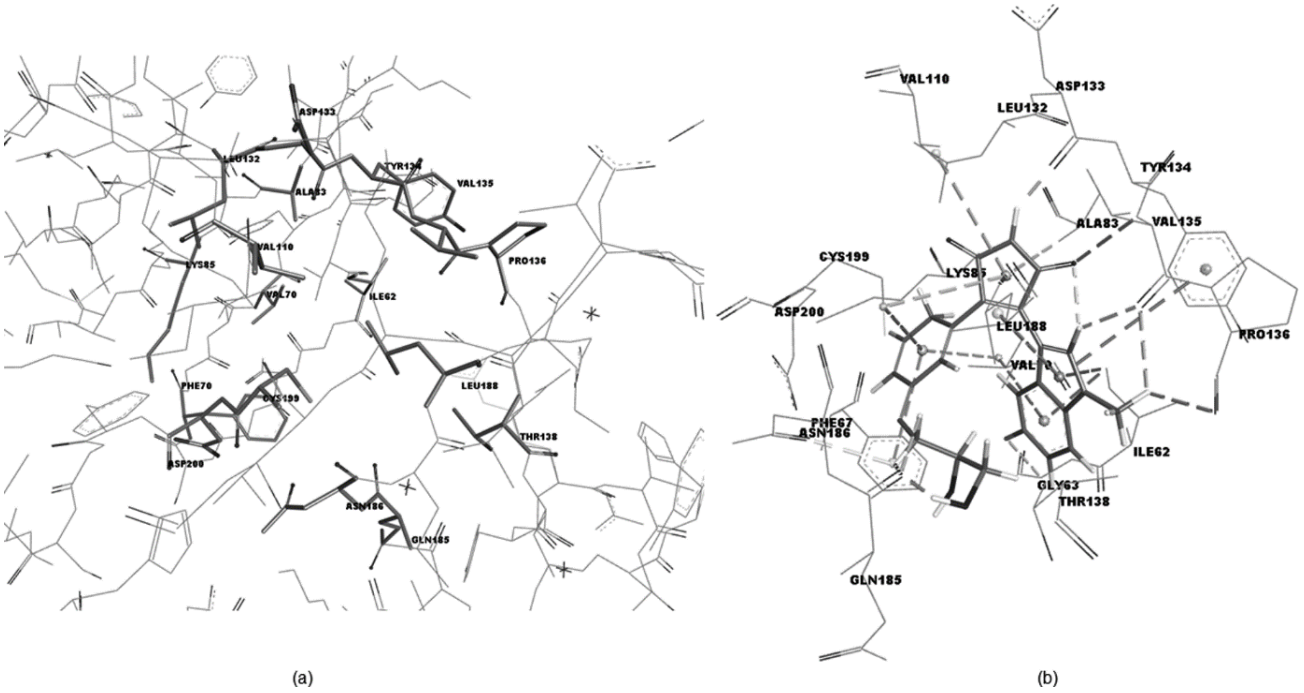

Fig. 4 – GSK-3β binding site view (PDB ID: 1R0E) (a); co-crystallized ligand 3-[3-(2,3-dihydroxy-propylamino)-phenyl]-4-(5-fluoro-1-methyl-1h-indol-3-yl)-pyrrole-2,5-dione (PDB ID: DFN) into binding site of GSK-3 (PDB ID:1R0E)(b).

The utility of this database consists in validated similarity cutoffs for the compounds displaying certain properties such as biological activity and selectivity,[57] *i.e.* the best 3D similarity screening rounds (query/coefficient) led to the conclusion to what cut-off value to use in virtual screening campaign to detect active GSK-3. The best performing coefficients Color Score and Scaled Color for query **2** recommended a cut-off value for activity -5.447 and 0.495 respectively.

Docking experiments including flexible ligand - rigid protein were performed with the help of FRED software (FRED 3.2.0.2: OpenEye Scientific Software, Santa Fe, NM. http://www.eyesopen.com)[58,59]. FRED requires a multiconformer ligand database which was initially prepared by generating ionization states and tautomers (pH = 7.2 ±0.2) involving LigPrep[60], which afterwards were subjected to conformer generation with OMEGA software[61-64]. The binding site was delineated using ligand location. Conformationally sampled ligands were docked into GSK-3β binding site (PDB ID:1R0E https://www.rcsb.org/structure/1r0e, resolution 2.25Å (Figure 4a)). The 3D structure of GSK-3β co-crystallized with 3-[3-(2,3-dihydroxy-

propylamino)-phenyl]-4-(5-fluoro-1-methyl-1h-indol-3-yl)-pyrrole-2,5-dione (PDB ID: DFN) was downloaded from PDB database (see Figure 4b).

GSK-3β ATP binding site is shown in Figure 4a, the residues which interact with ligand are highlighted. Visual inspection of the co-crystallized 3-[3-(2,3-dihydroxy-propylamino)-phenyl]-4-(5-fluoro-1-methyl-1h-indol-3-yl)-pyrrole-2,5-dione (PDB ID: DFN) with GSK-3β (PDB ID: 1R0E) (Figure 4b) reveals conventional hydrogen bond interactions with VAL135, ASP133, and GLN185, carbon hydrogen bond with PRO136, π-π hydrophobic interactions with PHE67, TYR134 and π-sigma hydrophobic interactions with CYS199, VAL110, LEU188, and ALA83.

In FRED, the best pose of the ligand is chosen based on a scoring function whose background consists in a shape-fitting algorithm (Figures 5-7). The 3D structures of representative GSK-3 inhibitors are shown in Figures 5(a), 6(a) and 7(a), whereas their complexes with the receptor are displayed in Figures 5(b), 6(b) and 7(b).

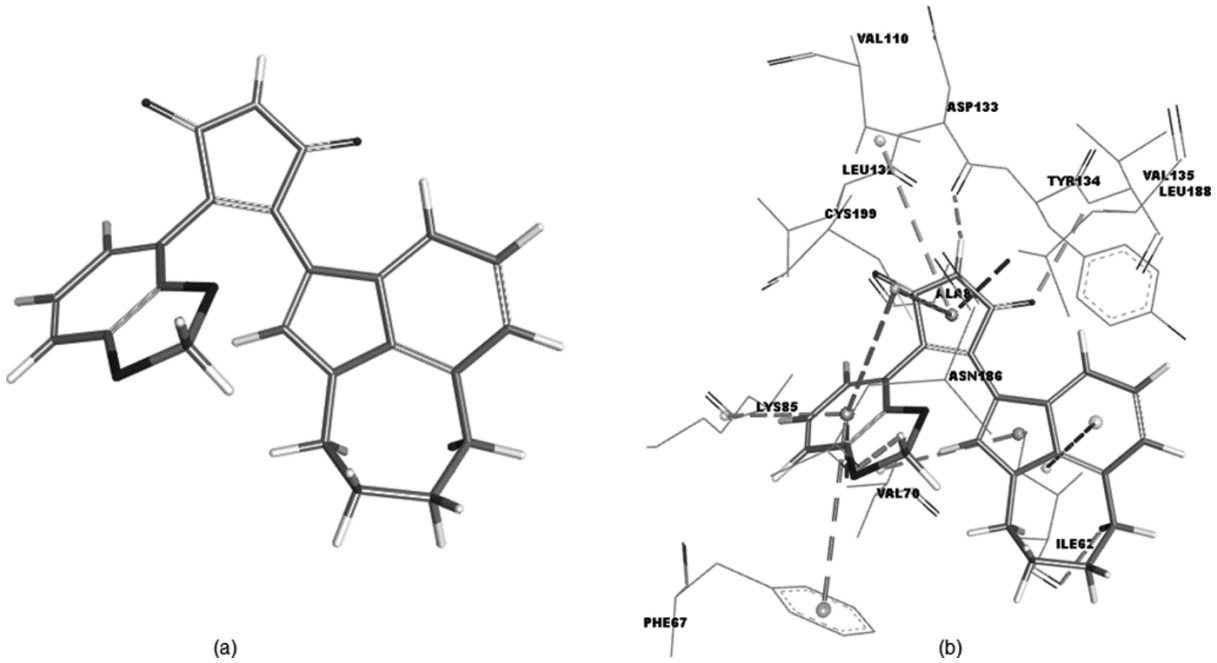

Fig. 5 – 3D Structure of 3-(2H-1,3-benzodioxol-4-yl)-4-{1,10-diazatricyclo[6.4.1.$0^{4,13}$]trideca-2,4(13),5,7-tetraen-3-yl}-2,5-dihydro-1H-pyrrole-2,5-dione (CHEMBL181774) (a); CHEMBL181774 docked into GSK-3 binding site (PDB ID:1R0E) (b).

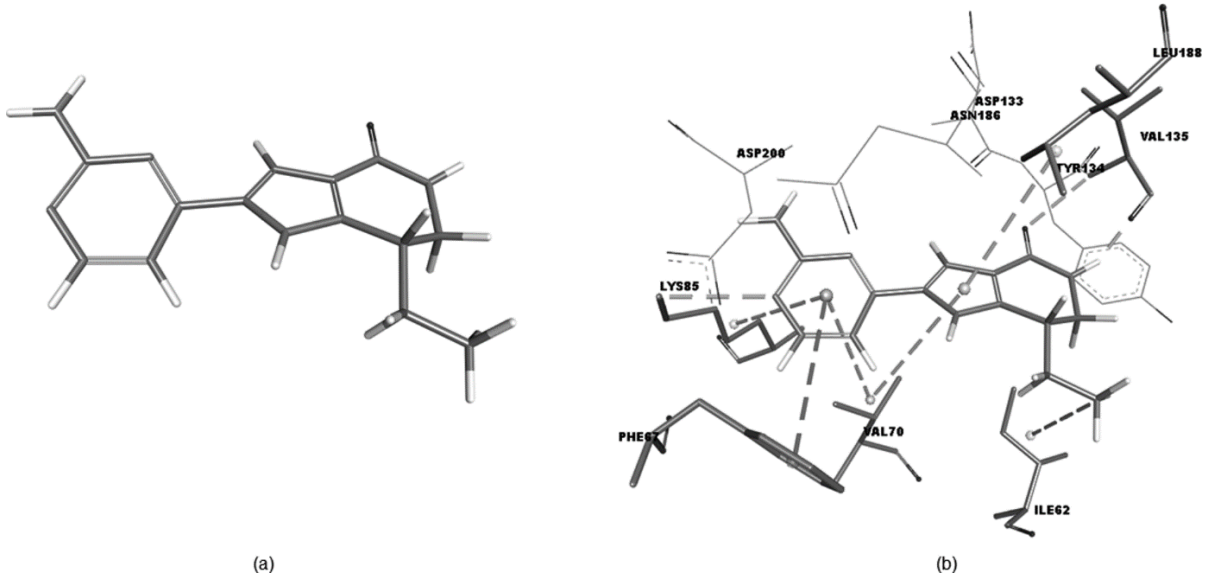

Fig. 6 – 3D Structure of (7S)-2-(2-aminopyrimidin-4-yl)-7-(2-fluoroethyl)-1H,4H,5H,6H,7H-pyrrolo[3,2-c]pyridin-4-one (CHEMBL524266) (a); docked complex of CHEMBL524266 and GSK-3 (PDB ID:1R0E) (b).

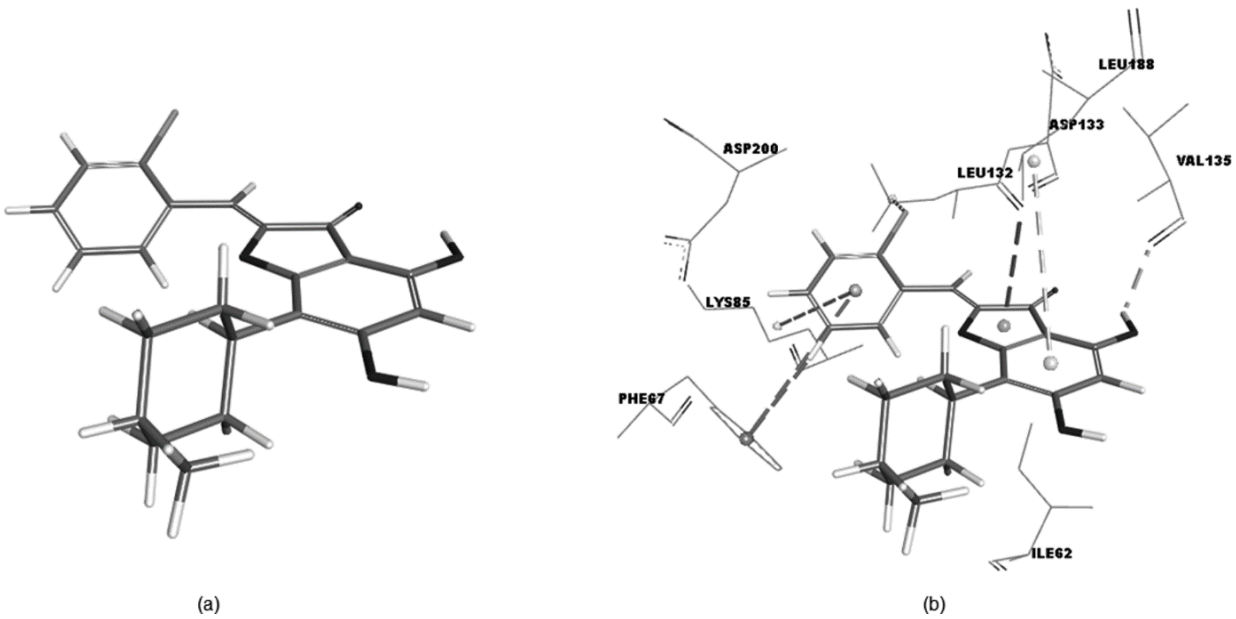

Fig. 7 – 3D conformation of 7-(2Z)-2-[(2-chlorophenyl)methylidene]-4,6-dihydroxy-7-(1-methylpiperidin-4-yl)-2,3-dihydro-1-benzofuran-3-one (CHEMBL48614) (a); docked pose of CHEMBL48614 into GSK-3 binding site (PDB ID:1R0E) (b).

The 3D structures of ligands display a planar central ring, *i.e.*, maleimide (CHEMBL181774) (Figure 5a), pyrrolo[3,2-c]pyridin-4-one (CHEMBL524266) (Figure 6a), and 2,3-dihydro-1-benzofuran-3-one (CHEMBL48614) (Figure 7a), whereas their substituents are positioned out of the plane to accommodate inside active site and maximize the interactions with binding site residues. For compound CHEMBL181774 (Figure 5b) the interactions resulted from docking are: conventional hydrogen bond interactions with VAL135, ASP133, carbon hydrogen bond with ILE62, π-π hydrophobic interactions with PHE67, π-sigma hydrophobic interactions with VAL70, LEU188, ILE62 and π-alkyl interactions with VAL110, ALA83, CYS199, VAL70, LYS85, and ILE62. The following interactions were observed for compound CHEMBL524266 (Figure 6b): conventional hydrogen bond interactions with VAL135, LYS85, π-π hydrophobic interactions with PHE67, π-alkyl interactions with VAL70, LEU188 and alkyl interactions with ILE62. We observed conventional hydrogen bond interactions with VAL135, π-π hydrophobic interactions with PHE67, π-sigma hydrophobic interactions with LEU188, PHE67, π-alkyl interactions with LYS85, LEU188 and LEU132 for compound CHEMBL48614 (Figure 7b). To sum up, the main interactions observed for the cocrystallized ligand 3-(2H-1,3-benzodioxol-4-yl)-4-{1,10-diazatricyclo[6.4.1.$0^{4,13}$]trideca-2,4(13),5,7-tetraen-3-yl}-2,5-dihydro-1H-pyrrole-2,5-dione were reproduced by the docked ligands CHEMBL181774, CHEMBL524266, and CHEMBL48614, demonstrating the reliability of the docking algorithm.

CONCLUSIONS

In the current work we engaged 2D and 3D similarity concepts, to investigate the activity/selectivity spectra of GSK-3 inhibitors. 3D Similarity metrics consisting in color field which accounts for pharmacophore areas of molecule scored more advantageously. For example, Ref Tversky Combo, Color Score and Scaled Color provided the best quality of 3D similarity rankings. Shape Tanimoto was identified as the second best criteria for active compounds enrichments. Exploiting the differences in terms of shape and pharmacophore variability will facilitate the design of novel small-molecule GSK-3 inhibitors. We expect that further development of methodology for actives prioritization will be of interest for the new paradigm of drug discovery - polypharmacology.

Acknowledgements. This project was financially supported by Project 1.2 of the Institute of Chemistry Timişoara of the Roumanian Academy. The authors thank Chemaxon Ltd. and OpenEye Scientific for providing academic license.

REFERENCES

1. J. Rauch, N. Volinsky, D. Romano and W. Kolch, *Cell. Commun. Signal.,* **2011**, *9*, 23.
2. P. Cohen, *Eur. J. Biochem.,* **2001**, *268*, 5001-5010.
3. P. Cohen and M. Goedert, *Nat. Rev. Drug. Discov.,* **2004**, *3*, 479-487.
4. J. A. Blair, D. Rauh, C. Kung, C-H. Yun, Q-W. Fan, H. Rode, C. Zhang, M. J. Eck, W. A. Weiss and K. M. Shokat, *Nat. Chem. Biol.*, **2007**, *3*, 229-238.

5. L. Xing, H. S. Shieh, S. R. Selness, R. V. Devraj, J. K. Walker, B. Devadas, H. R. Hope, R. P. Compton, J. F. Schindler, J. L. Hirsch, A. G. Benson, R. G. Kurumbail, R. A. Stegeman, J. M. Williams, R. M. Broadus, Z. Walden and J. B. Monahan, *Biochemistry*, **2009**, *48*, 6402-6411.
6. M. Hong, D. C. Chen, P. S. Klein and V. M. Lee, *J. Biol. Chem.*, **1997**, *272*, 25326-25332.
7. G. I. Welsh, C. M. Miller, A. J. Loughlin, N. T. Price and C. G. Proud, *FEBS. Lett*., **1998**, *421*, 125-130.
8. M. J. Hart, R. de los Santos, I. N. Albert, B. Rubinfeld and P. Polakis, *Curr. Biol.* **1998**, *8*, 573-581.
9. J. R. Woodget, *EMBO J.*, **1990**, *9*, 2431-2438.
10. K. Vougogiannopoulou, Y. Ferandin, K. Bettayeb, V. Myrianthopoulos, O. Lozach, Y. Fan, C. H. Johnson, P. Magiatis, A. L. Skaltsounis, E. Mikros and L. Meijer, *J. Med. Chem.*, **2008**, *5*, 16421-31.
11. D. G. Smith, M. Buffet, A. E. Fenwick, D. Haigh, R. J. Ife, M. Saunders, B. P. Slingsby, R. Stacey and R. W. Ward, *Bioorg. Med. Chem. Lett*., **2001**, *11*, 635-639.
12. Y. Mettey, M. Gompel, V. Thomas, M. Garnier, M. Leost, I. Ceballos-Picot, M. Noble, J. Endicott, J-M. Vierfond and L. Meijer, *J. Med. Chem.*, **2003**, *46*, 222-236.
13. H. Stukenbrock, R. Mussmann, M. Geese, Y. Ferandin, O. Lozach, T. Lemcke, S. Kegel, A. Lomow, U. Burk, C. Dohrmann, L. Meijer, M. Austen and C. Kunick, *J. Med. Chem.*, **2008**, *51*, 2196-2207.
14. L. Meijer, A. M. W. H. Thunnissen, A. W. White, M. Garnier, M. Nikolic, L-H. Tsai, J. Walter, K. E. Cleverly, P. C. Salinas, Y. Z. Wu, J. Biernat, E. M. Mandelkow, S. H. Kim and G. R. Pettit, *Chem. Biol.*, **2000**, *7*, 51-63.
15. M. P. Coghlan, A. A. Culbert, D. A. Cross, S. L. Corcoran, J. W. Yates, N. J. Pearce, O. L. Rausch, G. J. Murphy, P. S. Carter, Cox L. Roxbee, D. Mills, M. J. Brown, D. Haigh, R. W. Ward, D. G. Smith, K. J. Murray, A. D. Reith and J. C. Holder, *Chem. Biol.*, **2000**, *7*, 793-803.
16. D. A. E. Cross, A. A. Cubert, K. A. Chalmers, L. Facci, S. D. Skaper and A. D. Reith, *J. Neurochem.*, **2001**, *77*, 94-102.
17. A. A. Culbert, M. J. Brown, S. Frame, T. Hagen, D. A. Cross, B. Bax and A. D. Reith, *FEBS Lett.*, **2001**, *507*, 288-294.
18. D. S. Patel and P. V. Bharatam, *J. Comput. Aided Mol. Des.*, **2006**, *20*, 55-66.
19. A. R. Katritzky, L. M. Pacureanu, D. A. Dobchev, D. C. Fara, P. R. Duchowicz and M. Karelson, *Bioorg. Med. Chem.*, **2006**, *14*, 4987-5002.
20. N. Dessalew and V. B. Prasad, *Biophysical Chem.*, **2007**, *128*, 165-175.
21. N. Dessalew and P. V. Bharatam, *Eur. J. Med. Chem.*, **2007**, *42*, 1014-1027.
22. S. Prasanna, P. R. Daga, A. Xie and R. J. Doerksen, *J. Comput. Aided.Mol. Des.*, **2009**, *23*, 113-127.
23. K. H. Kim, I. Gaisina, F. Gallier, D. Holzle, S. Y. Blond and A. M. A. P. Kozikowski, *J. Mol. Model.*, **2009**, *15*, 1463-1479.
24. L. Pacureanu, A. Bora, L. Crisan and L. Kurunczi, *Stud. Univ. Babes-Bolyai Chem.,* **2010**, *LV*, 83-90.
25. L. Pacureanu, L. Crisan, A. Bora, S. Avram and L. Kurunczi, *Monatsh. Chem.*, **2012**, *143*, 1559-1573.
26. H. Pradeep and G. K. Rajanikant, *Mol. Divers.*, **2012**, *16*, 553-562.
27. L. Crisan, L. Pacureanu, A. Bora, S. Avram, L. Kurunczi and Z. Simon, *Cent. Eur. J. Chem.*, **2013**, *11*, 63-77.
28. A. Ritesh, J. Pratima, N. Subodh, R. Dikshit, B. Shyam and G. Swastika, *Med. Chem. Res.*, **2013**, *22*, 5504-5535.
29. L. Crisan, L. Pacureanu, A. Bora, S. Avram and L. Kurunczi, *Cent. Eur. J. Chem.*, **2013**, *11*, 1644-1656
30. L. Crisan, L. Pacureanu, S. Avram, A. Bora, S. Avram and L. Kurunczi, *J. Enz. Inhib. Med. Chem.*, **2014**, *29*, 599-610.
31. L. Quesada-Romero, K. Mena-Ulecia, W. Tiznado and J. Caballero, *PLOS ONE*, **2014**, *9*, e102212
32. L. Crisan, S. Avram, A. Bora, L. Kurunczi and L. Pacureanu, *Rev. Roum. Chim.,* **2015**, *60*, 183-188
33. L. Crisan, S. Avram and L. Pacureanu, *Mol. Divers.*, **2017**, *21*, 385-405.
34. Y. Kawasaki and E. Freire, *Drug Discov. Today,* **2011**, *16*, 985-990.
35. D. Schuster, *Drug Discov. Technol.*, **2010**, *7*, e205-e211.
36. D. Schuster, C. Laggner, T. M. Steindl and T. Langer, *Curr. Drug Discov. Technol.*, **2006**, *3*, 1-48.
37. D. Schuster, E. M. Maurer, C. Laggner, L. G. Nashev, T. Wilckens, T. Langer and A. Odermatt, *J. Med. Chem.*, *49*, 3454-3466.
38. S. G. Rohrer and K. Baumann, *J. Chem. Inf. Model.*, **2009**, *49*, 169-184.
39. N. Huang, B. K. Shoichet and J. J. Irwin, *J. Med.Chem.*, **2006**, *49*, 6789-6801.
40. J. P. Hughes, S. Rees, S. B. Kalindjian and K. L. Philpott, *Br. J. Pharmacol*., **2011**, *162*, 1239–1249.
41. I. N. Gaisina, F. Gallier, A. V. Ougolkov, K. H. Kim, T. Kurome, S. Guo, D. Holzle, D. N. Luchini, S. Y. Blond, D. D. Billadeau and A. P. Kozikowski, *J. Med. Chem.*, **2009**, *52*, 1853-1863.
42. T. A. Engler, S. Malhotra, T. P. Burkholder, J. R. Henry, D. Mendel, W. J. Porter, K. Furness, C. Diefenbacher, A. Marquart, J. R. Reel, Y. Li, J. Clayton, B. Cunningham, J. McLean, J. C. O'Toole, J. Brozinick, E. Hawkins, E. Misener, D. Briere, R. A. Brier, J. R. Wagner, R. M. Campbell, B. D. Anderson, R. Vaughn, D. B. Bennett, T. I. Meie and J.A. Cook, *Bioorg. Med. Chem. Lett.*, **2005**, *15*, 899-903.
43. A. P. Bento, A. Gaulton, A. Hersey, L. J. Bellis, J. Chambers, M. Davies, F. A. Krüger, Y. Light, L. Mak, S. McGlinchey, M. Nowotka, G. Papadatos, R. Santos and J. P. Overington, *Nucleic Acids Res.*, **2014**, *42*, 1083-1090.
44. T. Liu, Y. Lin, X. Wen, R. N. Jorissen and M. K. Gilson, *Nucleic Acids Res.*, **2007**, *35*, 198-201.
45. MarvinSketch (2017) version 17.18.0 ChemAxon. http://www. chemaxon.com.
46. Y. Wang, T. Suzek, J. Zhang, J. Wang, S. He, T. Cheng, B. A. Shoemaker, A. Gindulyte and S. H. Bryant, *Nucleic Acids Res.*, **2014**, *42*, 1075-1082.
47. FILTER 2.5.1.4: OpenEye Scientific Software, Santa Fe, NM.
48. S. I. Avram, L. Crisan, A. Bora, L. M. Pacureanu, S. Avram and L. Kurunczi, *Bioorg. Med. Chem*., **2013**, *21*, 1268-1278.
49. ROCS 3.2.1.4: OpenEye Scientific Software, Santa Fe, NM. http://www.eyesopen.com
50. P. C. D. Hawkins, A. G. Skillman and A. Nicholls, *J. Med. Chem.*, **2007**, *50*, 74-82.
51. J. Venhorst, S. Nunez, J. W. Terpstra and C.G. Kruse, *J. Med. Chem.,* **2008**, *51*, 3222-3229.
52. J.A. Hanley and B.J. McNeil, *Radiology*, **1982**, *143*, 29-36.
53. S. I. Avram, L. M. Pacureanu, A. Bora, L. Crisan, S. Avram and L. Kurunczi, *J. Chem. Inf. Model*., **2014**, *54*, 2360-2370.
54. A. N. Jain and A. Nicholls, *J. Comput. Aided. Mol. Des.,* **2008**, *22*,133-139.

55. A. C. Good, M. A. Hermsmeier and S. A. Hindle, *J. Comput. Aided. Mol. Des.,* **2004**, *18*, 529-536.
56. J. K. Lanctot, S. Putta, C. Lemmen and J. Green, *J. Chem. Inf. Comput.Sci*., **2003**, *43*, 2163-2169.
57. J. Srinivasen, A. Castellino, E. K. Bradley, J. R. Eksterowiez, P. D. J. Grootenhuis, S. Putta and R. V. Staton, *J. Med. Chem.,* **2002**, *45*, 2494-2500.
58. FRED Version 3.0.1 OpenEye Scientific Software Inc. Santa Fe NM, USA www.eyesopen.com.
59. M. McGann, J. Chem. Inf. Model., **2011**, *51*, 578-596.
60. LigPrep Version (**2011**) 2.5 Schrodinger LLC New York NY.
61. OMEGA Version 2.5.1.4 OpenEye Scientific Software Inc. Santa Fe NM, USA www.eyesopen.com.
62. P. C. D. Hawkins, A. G. Skillman, G. L. Warren, B. A. Ellingson and M. T. Stahl, *J. Chem. Inf. Model.*, **2010**, *50*, 572-584.
63. P. C. D. Hawkins and A. Nicholls, *J. Chem. Inf. Model.*, **2012**, *52*, 2919-2936.
64. J. Boström, J. R. Greenwood and J. Gottfries, *J. Mol. Graph. Model.*, **2003**, *21*, 449-462.